Poly(dehydroalanine): synthesis, properties and functional diversification of a fluorescent polypeptide

Isaac Benavides,[a†] Eric D. Raftery,[a†] Alexandra G. Bell,[a] Declan Evans,[a] Wendell A. Scott,[a] K. N. Houk,[a] and Timothy J. Deming[a,b,*]

[a] Department of Chemistry and Biochemistry, University of California, Los Angeles, CA 90095

[b] Department of Bioengineering, University of California, Los Angeles, CA 90095

[†] These authors contributed equally

Abstract Via the design of a new, soluble poly(S-alkyl-L-cysteine) precursor, a route was developed for successful preparation of long chain poly(dehydroalanine), A^{DH}, as well as the incorporation of dehydroalanine residues and A^{DH} segments into copolypeptides. Based on experimental and computational data, A^{DH} was found to adopt a previously unobserved 'hybrid coil' structure, which combines elements of 2_5-helical and 3_{10}-helical conformations. Analysis of the spectroscopic properties of A^{DH} revealed that it possesses strong inherent blue fluorescence, which may be amenable for use in imaging applications. A^{DH} also contains reactive electrophilic groups that allowed its efficient modification to functionalized polypeptides after reaction under mild conditions with thiol and amine nucleophiles. The combined structural, spectroscopic, and reactivity properties of A^{DH} make it a unique reactive and fluorescent polypeptide component for utilization in self-assembled biomaterials.

Introduction

Dehydroalanine (Dha) is an unsaturated amino acid that occurs naturally as a post-translational modification in peptides,[1,2] where it imparts unique conformational properties and electrophilic reactivity. Due to α,β-unsaturation, Dha residues prefer a planar conformation that can induce inverse γ-turns in peptides.[3] In one study, peptides containing three to six consecutive Dha residues were found to adopt extended 2_5-helical conformations, where each chain possesses a striking, essentially flat conformation due to ϕ and ψ angles being *ca.* $180°$ for each residue.[4] Dha residues are also potent electrophiles that react readily with thiol and amine nucleophiles.[5-8] Such reactions occur in the biosynthesis of cyclic peptide lantibiotics,[9] and have also been utilized as a strategy for site-specific functionalization of Dha residues in peptides and proteins.[10-15] In spite of the attractive conformation directing and reactivity properties of Dha, there has been no successful synthesis of long, repeating Dha sequences, i.e. poly(dehydroalanine), $\mathbf{A^{DH}}$.

The incorporation of multiple Dha residues into short peptides has been accomplished in a variety of examples.[16-19] The most significant were the flat peptides reported by Toniolo, where trimer through hexamer Dha peptides were synthesized and characterized.[4] In nearly all Dha containing peptides, the Dha residues were not incorporated during peptide synthesis, but were introduced after synthesis by conversion of precursor amino acids into Dha residues.[1,2,16-19] This strategy, which mimics the biosynthesis of Dha from serine residues,[1,2] is advantageous since it avoids the low nucleophilicity and instability of N-terminal enamine groups in Dha that hinder efficient peptide coupling (*vide infra*).[1,2] To date, a Dha hexamer is the longest repeat of Dha residues that has been reported.[4] In the 1950s, Sakakibara attempted to prepare long chain $\mathbf{A^{DH}}$ via the direct ring-opening polymerization of Dha N-carboxyanhydride (Dha NCA, Scheme 1).[20,21] These reactions, utilizing primary amine or strong base initiators, gave low conversions (< 35%) of monomer, possibly due to low reactivity of both monomer and enamine chain-ends, and gave polymers that contained < 10 mol% of Dha residues. Further studies

by Sakakibara revealed that a dominant reaction pathway was radical addition polymerization across the alkene bonds in Dha, either in monomer or polymer, resulting in loss of unsaturation (Scheme 1).[20-22] Direct synthesis of A^{DH} via NCA polymerization was found to be unsuccessful.
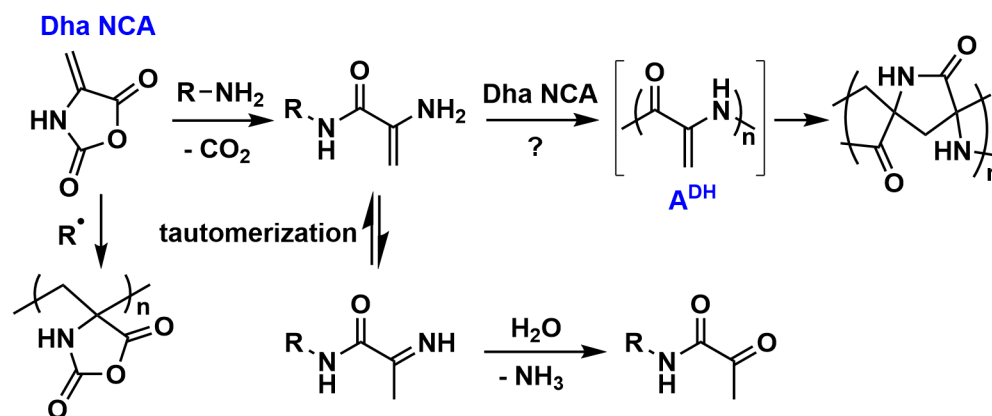

Scheme 1 Reactions previously reported for dehydroalanine N-carboxyanhydride (Dha NCA).[20-22] Brackets indicate that product was not isolated. A^{DH} = poly(dehydroalanine).

A^{DH} is a desirable biopolymer since it is expected adopt a chain conformation different from most other polypeptides (e.g. α-helices and β-sheets),[4,23,24] and this difference may lead to unique physical properties and assembled structures. A^{DH} would also be a potentially valuable precursor to functional polypeptides via post-polymerization reactions with various nucleophiles.[10-19] The α,β-unsaturation of Dha residues also permits peptide cleavage under mild acidic conditions,[1,2] which may be useful for applications where chain degradation is desirable. Here, we have circumvented longstanding challenges in the synthesis of A^{DH} by design of a soluble, readily prepared polypeptide precursor that can be efficiently modified to give A^{DH} of controlled length. The preparation of Dha containing block and statistical copolymers was also demonstrated using this approach. The Dha residues in these homo and copolypeptides were found to be efficiently derivatized by reaction with amine and thiol nucleophiles under mild conditions to yield the corresponding functionalized residues. Further, A^{DH} was found to adopt a previously unobserved 'hybrid coil' structure in both solvents and in the solid-state, and A^{DH} chains were also found to exhibit inherent blue fluorescence. The controlled synthesis of A^{DH} containing

polypeptides and the unique properties of A^{DH} reported here are a promising combination for development of chemically reactive and 'label-free' fluorescent polypeptide materials.

Results and Discussion

Since there have been considerable improvements in NCA polymerization methodology[25] since Sakakibara's work in the 1950s, we first sought to re-evaluate the polymerization of Dha NCA to determine if preparation of A^{DH} via this route was feasible (Scheme 2). Using a monomer to initiator ratio of 30 to 1, and either THF or DMF as solvent, polymerizations of Dha NCA were initiated using either $nBuNH_2$ or $Co(PMe_3)_4$ initiator[26] under air-free and anhydrous conditions at 20 °C. In all four polymerizations, Dha NCA consumption was sluggish as compared to other NCA monomers, and only small fractions of monomer were consumed after 24h (see supporting information, SI). Reaction mixtures were diluted with water, and after no observation of precipitates the samples were then dialyzed against water to remove small molecules followed by lyophilization. Oligomeric products were then obtained as off-white solids in poor yields (11 to 16% for $nBuNH_2$, and 27 to 42% for $Co(PMe_3)_4$). Notably, only the product from $nBuNH_2$ initiation in DMF showed resonances in its ^1H NMR spectrum assignable as alkene protons, and all products contained resonances consistent with aliphatic protons that should not be present in A^{DH} (see SI). Solid-state FTIR analysis of the samples also gave spectra that were not consistent with A^{DH} (*vide infra*, see SI Figure S1). Overall, in agreement with Sakakibara's findings,[20-22] and the known poor reactivity and stability issues of enamine groups in Dha (Scheme 1),[1,2] our results confirmed that direct formation of A^{DH} via polymerization of Dha NCA was not feasible.
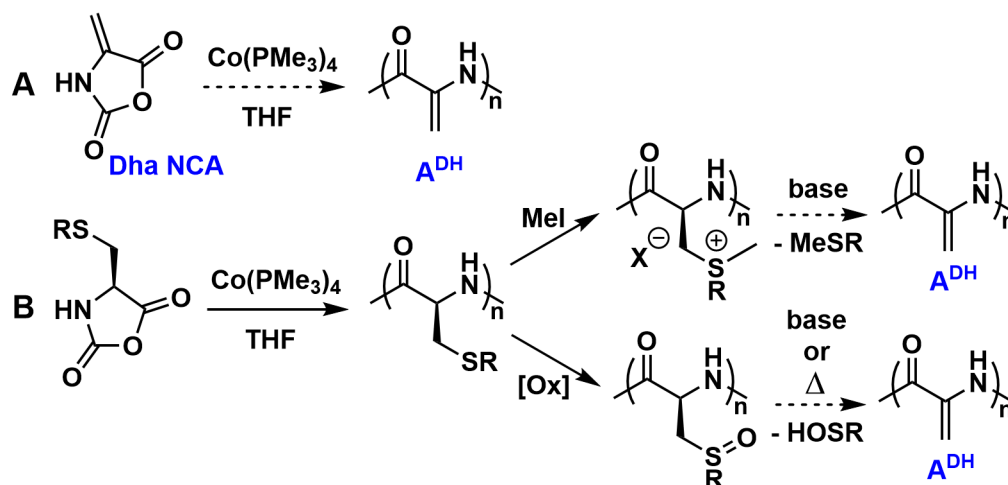
Scheme 2 Potential synthetic routes to poly(dehydroalanine), A^{DH}. A) Direct polymerization of Dha NCA. B) Preparation of a poly(S-alkyl-L-cysteine) precursor followed by thioether alkylation or oxidation and subsequent base catalyzed or thermal elimination. R = alkyl group.

Consequently, we sought to develop an alternative route to A^{DH} based on a precursor polypeptide (Scheme 2), similar to methods used to introduce Dha residues into peptides and proteins. As shown in Scheme 3, many routes have been utilized to convert amino acid precursors into Dha residues in peptides and proteins.[1,2,16-19,27-35] The most economical of these strategies rely on precursors based on natural cysteine or serine residues. While the methods in Scheme 3 work well for peptides and proteins, these molecules either contain few Dha residues or consist of short chains such that the solubility of the molecules is not compromised by incorporation of either precursor or Dha residues.[1,2,4,16-19] For polypeptides, a major challenge in development of a A^{DH} precursor is that nearly all derivatives of long chain poly(cysteine) or poly(serine) adopt stable β-sheet conformations, and consequently have low solubility in most solvents.[36] The poor solubility of these polypeptides prohibits controlled synthesis of high molecular weight chains, and also can hinder their conversion to A^{DH}.
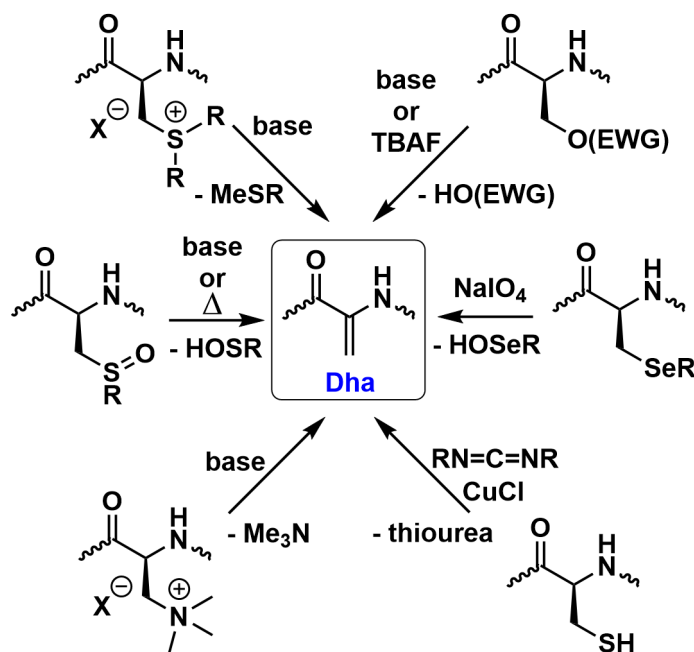
Scheme 3 Synthetic routes to Dha residues in peptides and proteins.[1,2,16-19,27-35] R = alkyl group. EWG = -Tosyl, -C(O)OR, or -PO$_3{}^{2-}$. TBAF = tetrabutylammonium fluoride.

To address this challenge, we sought to develop a viable precursor to **A^{DH}** that possesses good solubility in solvents used for NCA polymerization to allow for controlled chain growth. Guided by prior observations, our efforts focused on derivatives of poly(L-cysteine). While most poly(L-cysteine) derivatives form poorly soluble β-sheets, e.g. protected poly(S-carboxyalkyl-cysteines),[37-41] protected poly(S-aminoalkyl-cysteines),[42-43] and poly(S-alkyl-cysteines),[44-48] we noted two examples had been reported that instead favor the soluble α-helical conformation. The first was poly(S-(L-menthyloxycarbonylmethyl)-L-cysteine),[49] and the second was a series of acetyl protected, monosaccharide functionalized poly(S-alkyl-L-cysteines) reported by our group.[50] Due to the lack of interchain H-bonding that would occur in β-sheet conformations,[36] these α-helical poly(L-cysteine) derivatives were found to possess good solubility in organic solvents useful for NCA polymerization (e.g. THF), which allows preparation of high molecular weight chains.

We observed that a common feature of these α-helical poly(L-cysteine) derivatives was the presence of sterically demanding groups (i.e. menthyl and tetra-acetyl monosaccharide) at the ends of the

side chains, which may be responsible for their conformational preference. This observation led to a design concept for a simplified α-helical poly(L-cysteine) derivative to serve as an efficient precursor to **A^DH**. While poly(S-(benzyloxycarbonylmethyl)-L-cysteine) is well-known to adopt stable β-sheet conformations that precipitate or gel during polymerization,[37-39] we hypothesized that replacement of the benzyl groups with groups that were more sterically demanding could give α-helical polypeptides that would be soluble to high degrees of polymerization.[50] Further, although the hindered ester in poly(S-(L-menthyloxycarbonylmethyl)-L-cysteine) is difficult to hydrolyze, other alkoxycarbonyl protecting groups may be more readily removed to give poly(S-carboxymethyl-L-cysteine), **C^CM**, which is water soluble when the carboxylates are deprotonated at pH > 4.[51-53] A water soluble poly(S-carboxyalkyl-L-cysteine) precursor is desirable since both sulfonium and sulfoxide routes for its conversion to **A^DH** could be conducted under mild conditions in aqueous media (Scheme 2).[9,16,19,29,30,54] Hence, we designed and prepared a new L-cysteine based polypeptide, poly(S-(*tert*-butoxycarbonylmethyl)-L-cysteine), **C^BCM**, containing the sterically demanding *tert*-butyl group to both favor helical conformations and allow facile deprotection.
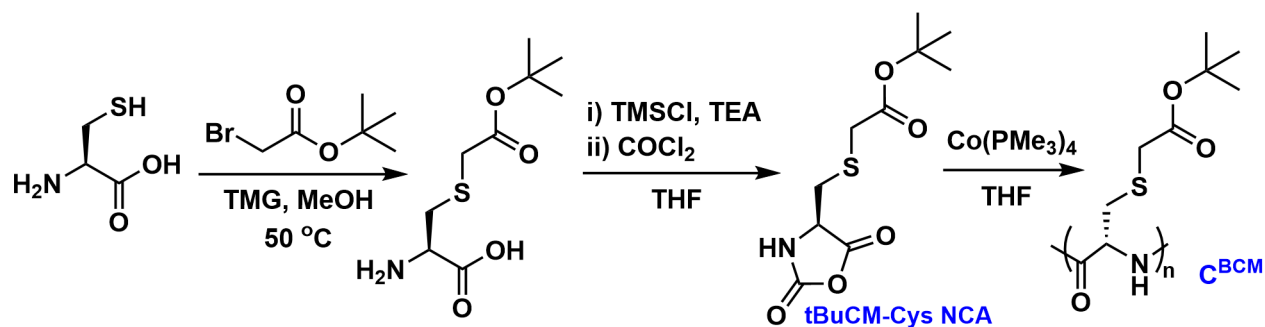
Scheme 4 Preparation of S-(*tert*-butoxycarbonylmethyl)-L-cysteine N-carboxyanhydride, *t*BuCM-Cys NCA, and poly(S-(*tert*-butoxycarbonylmethyl)-L-cysteine), **C^BCM**. TMG = tetramethylguanidine.

L-Cysteine was converted to S-(*tert*-butoxycarbonylmethyl)-L-cysteine using established procedures,[55] and this amino acid was then converted to its corresponding NCA under conditions that avoid the formation of HCl so that the *tert*-butyl esters remained intact (Scheme 4).[56] The resulting

purified S-(*tert*-butoxycarbonylmethyl)-L-cysteine NCA, *t*BuCM-Cys NCA, was found to readily polymerize using Co(PMe₃)₄ in THF at 20 °C,[26] giving **C^BCM** that remained soluble in the reaction mixture. Chain lengths of **C^BCM** were readily controlled by variation of monomer to initiator ratio (Figure 1a), and molecular weight distributions remained narrow and monomodal (Figure 1a,b). Further, block and statistical copolypeptides of *t*BuCM-Cys NCA with a model co-monomer *tert*-butyl-L-glutamate NCA, *t*Bu-Glu NCA, were readily prepared (Table 1, See SI Schemes S1 and S2, Figures S2 and S3, and Table S1), which altogether confirmed the ability of *t*BuCM-Cys NCA to undergo living polymerization. Thus, our design of **C^BCM** was successful in preventing formation of insoluble β-sheet aggregates. Additional conformational data for **C^BCM** were obtained from FTIR and circular dichroism studies (Figure 1c,d), which were consistent with this polypeptide adopting an extended chain conformation.[57] The spectra of **C^BCM** show features similar to those observed for poly(α-GalNAc-L-serine), which has been shown to adopt a highly extended helical conformation.[58]
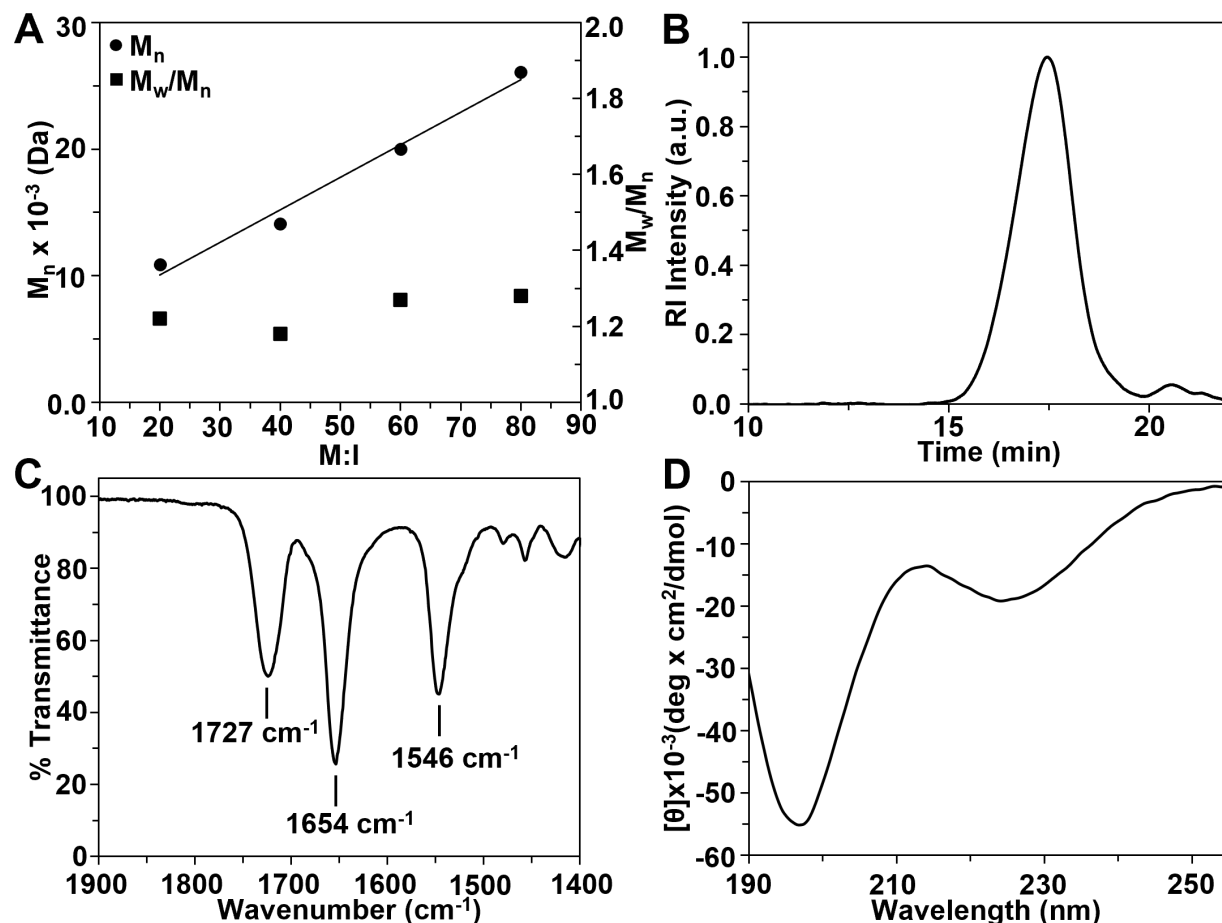
Figure 1 A) Variation in molecular weight (M_n, determined by ^{1}H NMR) and dispersity (M_w/M_n, determined by GPC) of $\mathbf{C^{BCM}}$ as a function of monomer to Co(PMe$_3$)$_4$ initiator ratio (M:I) in THF at 20 °C. B) GPC trace of $\mathbf{C^{BCM}}_{77}$ in HFIP containing 0.5% (w/w) KTFA. C) Solid-state FTIR spectrum of the amide region for $\mathbf{C^{BCM}}_{77}$. The Amide I and II bands at 1654 and 1546 cm^{-1} are consistent with a helical conformation.[57] The band at 1727 cm^{-1} is the carbonyl stretch of the *tert*-butyl ester groups. D) CD spectrum of $\mathbf{C^{BCM}}_{77}$ in HFIP. Bands at 197 and 224 nm suggest that the polymer is adopting an extended helical conformation in this solvent.[58]

Table 1 Synthesis of diblock copolypeptides using Co(PMe₃)₄ initiator in THF.

Monomer Feed Compositions		First Segment[b]			Diblock copolymer[c]			
First Monomer[a]	Second Monomer[a]	M_n	DP	Đ	M_n	DP	Đ	Yield(%)[d]
40 *t*Bu-Glu NCA	40 *t*BuCM-Cys NCA	20,200	88	1.28	42,400	173	1.29	96
40 *t*BuCM-Cys NCA	40 *t*Bu-Glu NCA	20,200	77	1.17	41,300	169	1.17	93

[a]First and second monomers added stepwise to the initiator at 20 °C; number indicates equivalents of monomer per Co(PMe₃)₄. [b]Molecular weight (M_n) and dispersity ($Đ = M_w/M_n$) after polymerization of the first monomer determined by ¹H NMR and GPC. [c]Molecular weight and dispersity after polymerization of the second monomer determined by ¹H NMR and GPC. [d]Total isolated yield of deprotected diblock copolypeptide as the sodium salt. DP = number average degree of polymerization.

With successful controlled preparation of the soluble polypeptide precursor **C**[BCM], the next step was to attempt to convert this into **A**[DH]. As shown in Scheme 2, we considered both alkylation and oxidation routes to convert **C**[BCM] to **A**[DH]. Some efforts were made initially to directly convert organic soluble **C**[BCM] to **A**[DH], but these suffered from poor yields and negligible formation of **A**[DH]. Consequently, **C**[BCM] was readily deprotected using trifluoroacetic acid (TFA) to obtain, after neutralization, the water soluble poly(S-carboxymethyl-L-cysteine), **C**[CM], as its sodium salt (Scheme 5). The thioether groups in **C**[CM] could either be fully oxidized (see SI Scheme S3) or fully methylated (Scheme 5) under mild conditions in aqueous media, similar to other thioether containing polypeptides.[59,60] While attempts to eliminate the sulfoxide groups at pH 8.0 and 37 °C were found to give only *ca*. 8% conversion to Dha residues (see SI), the elimination of sulfonium groups was found to proceed rapidly at pH 8.0 and 37 °C to give **A**[DH] in high conversion and yield (Scheme 5).[61,62] Elimination occurred so readily at this pH that the sulfonium product was not isolated, and hydrophobic **A**[DH] precipitated directly from the reaction mixture. Thus, methylation of **C**[CM] was determined to be the most efficient method for preparation of **A**[DH] (Scheme 5). Note that small amounts of butylated hydroxytoluene (BHT) were added to these

reactions (0.01 mol% relative to each Dha residue) in order to inhibit radical induced decomposition of the reactive Dha functional groups. Also, as the N-terminal groups of the $\mathbf{A^{DH}}$ chains are enamines (see SI Scheme S4), it is expected that these will be hydrolyzed to N-terminal pyruvoyl groups under the basic conditions used for synthesis (Scheme 1, see SI Scheme S4).
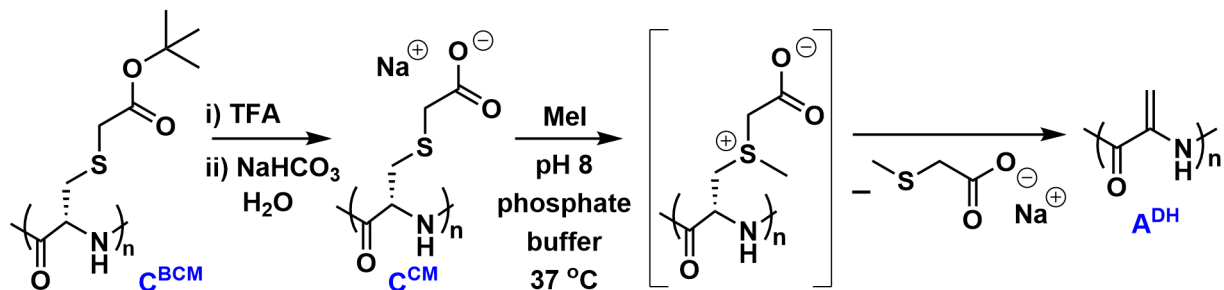
Scheme 5 Deprotection of $\mathbf{C^{BCM}}$ to give poly(S-carboxymethyl-L-cysteine), $\mathbf{C^{CM}}$, and conversion of $\mathbf{C^{CM}}$ to $\mathbf{A^{DH}}$ via methylation and subsequent base catalyzed elimination. Brackets indicate that the intermediate was not isolated.

Samples of $\mathbf{A^{DH}}$ formed as off-white precipitates that were insoluble in water, but were found to disperse well in DMSO, TFA and hexafluoroisopropanol (HFIP) solvents. GPC analysis of $\mathbf{A^{DH}}$ in HFIP showed a monomodal peak (Figure 2a) with retention time similar to the $\mathbf{C^{CM}}$ precursor. This result, combined with measurement of chain lengths of $\mathbf{C^{CM}}$ and $\mathbf{A^{DH}}$ segments relative to 1 kDa PEG endgroups via ^{1}H NMR integration (see SI) confirmed that no chain cleavage occurred during conversion of $\mathbf{C^{CM}}$ to $\mathbf{A^{DH}}$. The dispersity of $\mathbf{A^{DH}}$ ($Đ = 2.3$, Figure 2a) was greater than the $\mathbf{C^{CM}}$ precursor ($Đ \sim 1.2$), but this was likely due to partial aggregation of $\mathbf{A^{DH}}$ chains, which was observed in HFIP as well as all other solvents tested (*vide infra*). The composition of $\mathbf{A^{DH}}$ samples was confirmed by ^{1}H and ^{13}C NMR spectroscopy, as well as FTIR analysis (Figure 2). Contrary to the oligomers obtained above from attempted Dha NCA polymerizations, the ^{1}H NMR spectrum of $\mathbf{A^{DH}}$ derived from the $\mathbf{C^{CM}}$ sulfonium precursor showed the expected resonances for the alkene and amide protons of Dha residues (Figure 2b).[4] The solid-state CP-MAS ^{13}C NMR spectrum of $\mathbf{A^{DH}}$ was also consistent with the expected structure, with resonances for carbonyl and alkene carbons (Figure 2c) that were analogous to those observed in Dha

containing small molecules.[63] Observation of two resonances for each carbon likely reflects different residue conformations in the solid-state (*vide infra*). Finally, the FTIR spectrum of $\mathbf{A^{DH}}$ contained bands at 1681, 1656 and 1492 cm^{-1} consistent with Amide I and Amide II vibrations, as well as bands at 1625 and 902 cm^{-1} that are consistent with an alkene stretch[64] and an alkene out of plane bend[65] in $\mathbf{A^{DH}}$, respectively (Figure 2d, see SI Figures S4 and S5). Altogether, these data confirm the successful preparation of long chain $\mathbf{A^{DH}}$.
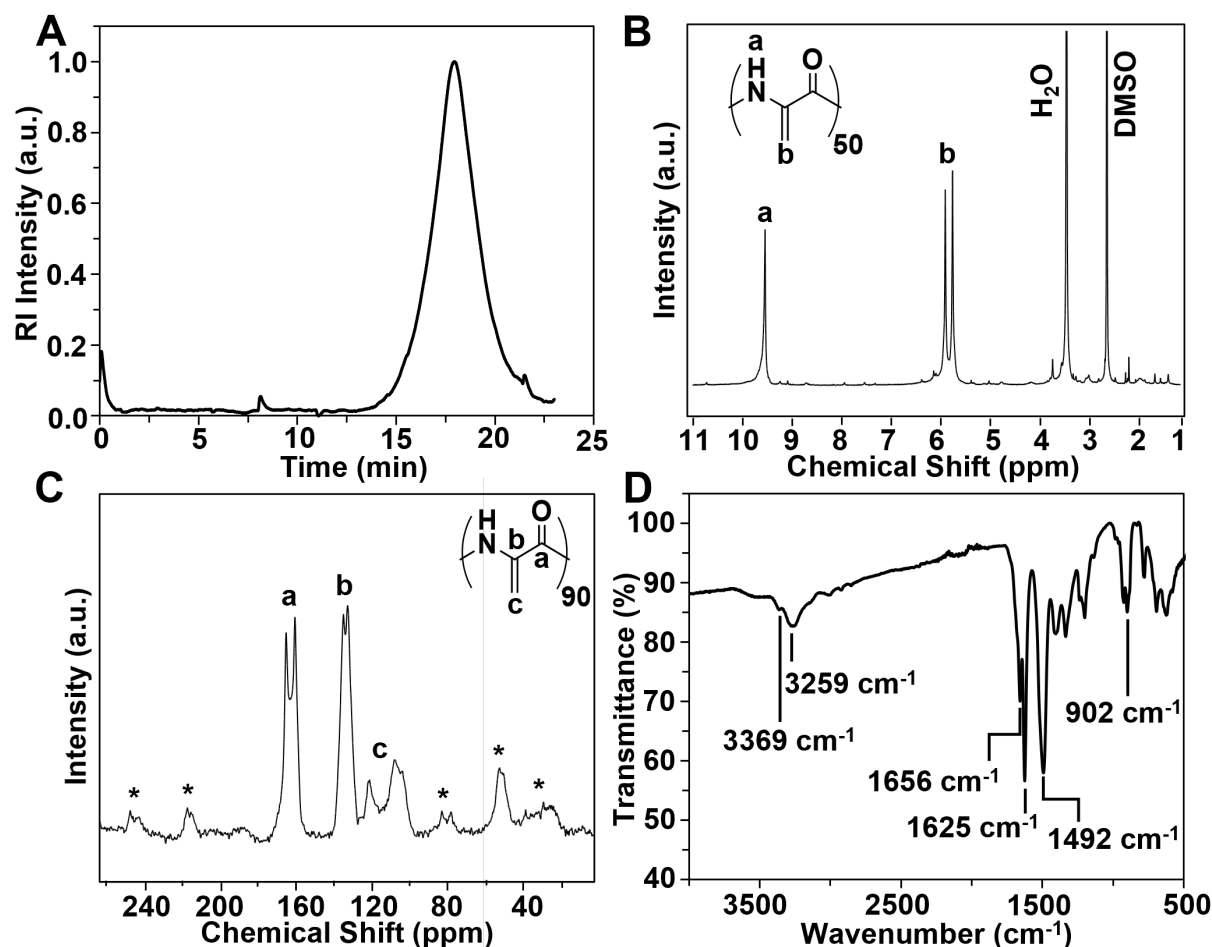

Figure 2 Characterization data for $\mathbf{A^{DH}}$. A) GPC trace of $\mathbf{A^{DH}_{72}}$ in HFIP containing 0.5% (w/w) KTFA ($Đ$ = 2.3). B) ^{1}H NMR spectrum of $\mathbf{A^{DH}_{50}}$ in DMSO-d_6. C) Solid-state CP-MAS ^{13}C NMR spectrum of $\mathbf{A^{DH}_{90}}$. Asterisks indicate spinning side bands. D) Solid state FTIR spectrum of $\mathbf{A^{DH}_{68}}$. The band at 902 cm^{-1} is consistent with alkene =C-H out of plane bends in $\mathbf{A^{DH}}$.[65] The band at 1625 cm^{-1} is consistent with

12

alkene stretches in $\mathbf{A^{DH}}$.[64] The bands at 1656 and 1492 cm^{-1} are consistent with Amide I and Amide II vibrations for peptides in the extended 2_5-helical conformation.[66]

In addition to helping confirm its composition, FTIR analysis of $\mathbf{A^{DH}}$ also provided valuable insights into the chain conformation of $\mathbf{A^{DH}}$. As mentioned in the introduction, Toniolo and coworkers discovered that short oligomers of Dha adopt the flat 2_5-helical conformation,[4] and this group has also pioneered the study of other peptide motifs that adopt this structure.[66] These investigations led to the identification of signature FTIR bands for 2_5-helices, similar to those that are well known for α-helices, 3_{10}-helices and β-sheets.[67] Specifically, Toniolo and coworkers noted that peptides in the 2_5-helical conformation possess a strong Amide II band at *ca.* 1490 cm^{-1} and split Amide I bands at *ca.* 1675 and 1650 cm^{-1}, where the Amide II band has greater intensity than the Amide I bands.[66] This pattern is distinct from the Amide bands of all other peptide conformations and is present in the $\mathbf{A^{DH}}$ samples prepared here, both in solid-state and in HFIP (Figure 2d, see SI Figures S4 and S5), and strongly suggests that long chain $\mathbf{A^{DH}}$ at least partially adopts the 2_5-helical conformation.

However, a discrepancy exists between the 2_5-helical hexamer of Dha and $\mathbf{A^{DH}}$ in the FTIR N-H stretching region, where this band occurs at *ca.* 3380 cm^{-1} for the hexamer of Dha[4] and two bands appear for $\mathbf{A^{DH}}$ at 3369 and 3259 cm^{-1} (Figure 2d, see SI Figure S5). The smaller $\mathbf{A^{DH}}$ N-H stretch at 3369 cm^{-1} is consistent with the 3380 cm^{-1} band for the hexamer of Dha since this band is known to shift to lower wavenumbers as the number of Dha repeats increases,[4] and is due to weak intra-residue H-bonding in the 2_5-helical conformation.[66] On the other hand, the larger $\mathbf{A^{DH}}$ N-H stretch at 3259 cm^{-1} indicates much stronger H-bonding than previously found in peptides with a 2_5-helical conformation.[66] A possible explanation for this additional N-H band may be the partial folding or association of longer chains in $\mathbf{A^{DH}}$ via inter-residue H-bonding (*vide infra*). Such folding would likely lead to conformational distortion of chain segments from the fully extended 2_5-helical conformation, and could also explain the presence of two sets of resonances observed in the solid-state CP-MAS ^{13}C NMR spectra (Figure 2c). Consistent with

this hypothesis, weak shoulders are present in the Amide region of the $\mathbf{A^{DH}}$ FTIR spectra at *ca.* 1697 and 1519 cm^{-1} (see SI Figure S5), which suggests that some portions of $\mathbf{A^{DH}}$ chains adopt conformations other than the fully extended 2$_5$-helix in the solid state and in HFIP (*vide infra*).

To understand the conformational properties of $\mathbf{A^{DH}}$ in more detail, we performed computational analysis using density functional theory (DFT). Geometry optimizations and frequency calculations were performed at the B3LYP-D3/6-31G(d) level of theory and single point energies were calculated at the ωB97X-D/def2TZVP level of theory using the SMD (solvation model density) for dimethyl sulfoxide (see SI). Models of $\mathbf{A^{DH}}$ with varying chain lengths were optimized in both the 2$_5$-helical conformation and the 3$_{10}$-helical conformation (Figure 3a). The 3$_{10}$-helix was included here since it has also been proposed to be a stable conformation for $\mathbf{A^{DH}}$.[23,24] We found the 2$_5$-helical conformation to be clearly preferred in the shorter chains, with a free energy difference of 8.1 kcal/mol between the favored 2$_5$-helical conformation and the higher energy 3$_{10}$-helical conformation of $\mathbf{A^{DH}_4}$ (Figure 3b). This energy difference varies linearly with polymer-length, and the 3$_{10}$-helical conformation becomes preferred in the longer chains $\mathbf{A^{DH}_{16}}$, $\mathbf{A^{DH}_{20}}$, and $\mathbf{A^{DH}_{24}}$.

To better understand this trend, we performed noncovalent interaction (NCI) analyses on the DFT-optimized models (Figure 3c). The NCI calculations show that the 2$_5$-helical conformation is stabilized by weak dispersion interactions between the methylidene groups of the side-chain and the amide groups of the backbone. Additionally, the linearized backbone dihedrals allow for weak intra-residue hydrogen bonding between the backbone carbonyl oxygens and amide hydrogens, sometimes referred to as C5 hydrogen bonds.[68-72] These noncovalent interactions, along with the extended π-electron conjugation, make the 2$_5$-helical conformation more stable in shorter $\mathbf{A^{DH}}$ chains. The 3$_{10}$-helical conformation is stabilized by dispersion interactions along the helix, and inter-residue hydrogen bonding between the *i* and *i+3* residue positions. These inter-residue hydrogen bonds have more linear N-H-O angles, making them stronger than the intra-residue hydrogen bonds observed in the 2$_5$-helical conformation. As the $\mathbf{A^{DH}}$

chain length increases, these inter-residue hydrogen bonds become more abundant, leading to the preference for the 3_{10}-helical conformation in these molecules.
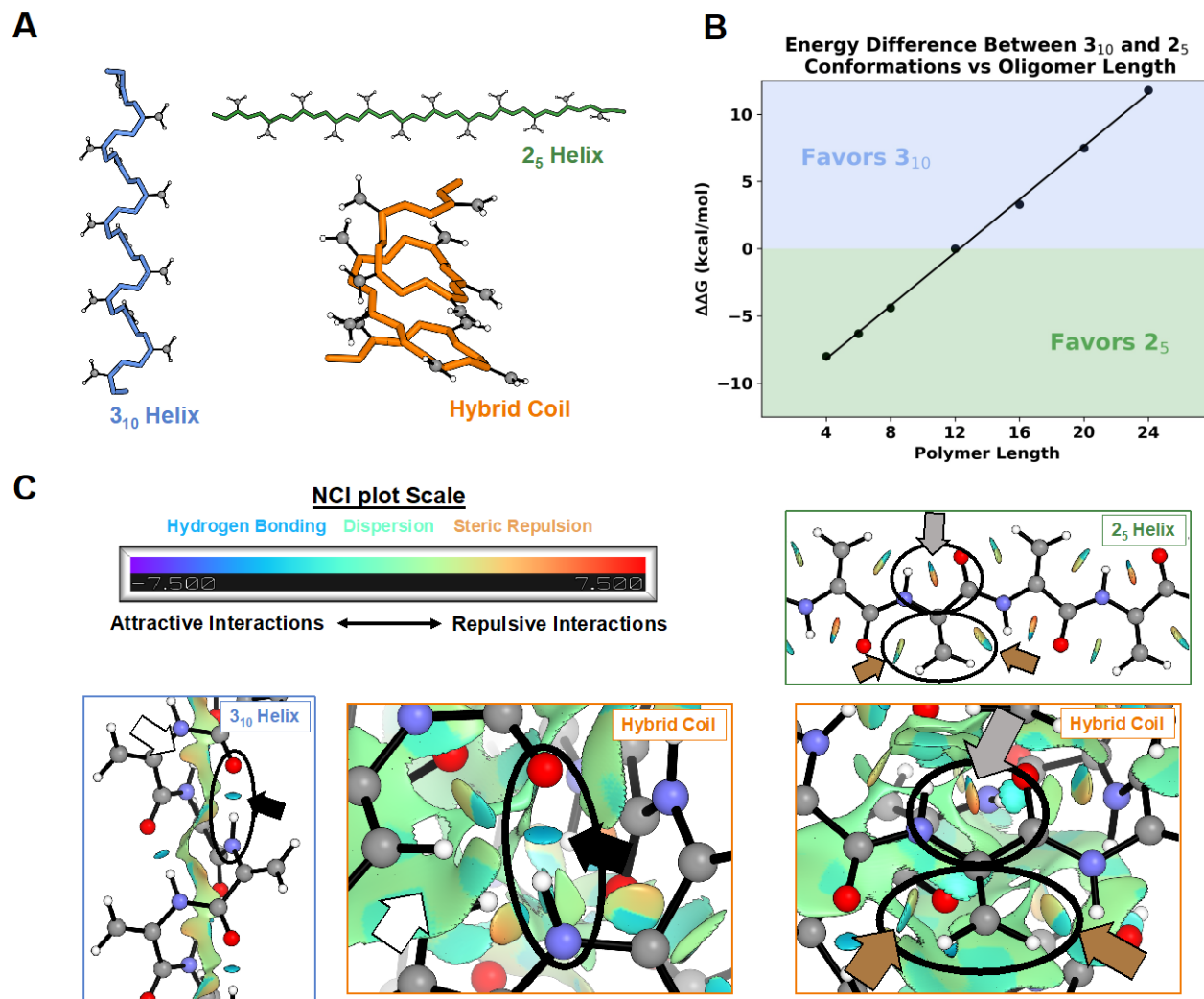

Figure 3 Computational analysis of $\mathbf{A^{DH}}$ conformations. (A) Backbone traces of DFT-optimized models of $\mathbf{A^{DH}_{12}}$. The 2_5-helix conformation is shown in green, the 3_{10}-helix conformation is shown in blue, and the hybrid coil conformation is shown in orange. (B) Plot of polymer length versus the difference in free energy between the 2_5-helix and 3_{10}-helix conformations. Short repeats $\mathbf{A^{DH}_4}$, $\mathbf{A^{DH}_6}$, and $\mathbf{A^{DH}_8}$ favor the 2_5-helix conformation. Longer repeats $\mathbf{A^{DH}_{16}}$, $\mathbf{A^{DH}_{20}}$, and $\mathbf{A^{DH}_{24}}$ favor the 3_{10}-helix conformation. The energies are equivalent in $\mathbf{A^{DH}_{12}}$. (C) NCI plots of the DFT optimized structures of $\mathbf{A^{DH}_{12}}$. Scale is shown for colors that represent attractive interactions like hydrogen bonding and dispersion, along with repulsive

interactions like steric repulsion. Weak dispersion interactions are observed along the helix in the 3_{10}-helix conformation and throughout the backbone in the hybrid coil conformation (white arrows). Additional weak dispersion interactions are observed between the sidechain and backbone in the 2_5-helix conformation and for flat residues in the hybrid coil conformation (brown arrows). Inter-residue hydrogen bonding is observed between *i* and *i+3* residue positions in the 3_{10}-helix conformation and throughout the hybrid coil conformation (black arrow). Intra-residue hydrogen bonding is observed between the backbone carbonyl oxygens and amide hydrogens in the 2_5-helix conformation and in flat residues in the hybrid coil conformation (gray arrow).

In addition to the 2_5-helical and 3_{10}-helical conformations, we explored other possible conformations of $\mathbf{A^{DH}_{12}}$ using CREST, a conformational search algorithm which uses meta-dynamics to rapidly explore conformational space.[73] This led to the discovery of a third conformation type, where some residues adopt the 2_5-helical conformation, but other residues have bends in either the φ or ψ dihedral angles that cause the chain to fold into a loose coil-like structure (Figure 3a). NCI plots show this new "hybrid coil" conformation has characteristics of both the 2_5-helical and 3_{10}-helical conformations (Figure 3c). The nearly linearized backbone of many residues allows extended π-electron conjugation and the same intra-residue hydrogen bonding that stabilizes the 2_5-helical structure. The hybrid coil structure also allows for increased dispersion along the backbone and the same inter-residue hydrogen bonds that stabilize the 3_{10}-helical conformation. The free energy difference of 2.6 kcal/mol in favor of the hybrid coil conformer compared to either the 2_5-helical and 3_{10}-helical conformations of $\mathbf{A^{DH}_{12}}$ shows that this conformation is clearly preferred, although $\mathbf{A^{DH}_{12}}$ chains may exist in an equilibrium between conformations in solution. Altogether, this new hybrid coil conformation with elements of both 2_5-helical and 3_{10}-helical conformations fits well with our experimental data that shows evidence of both intra- and inter-chain H-bonding, and is the best model for the conformation of long $\mathbf{A^{DH}}$ chains.

When further investigating the properties of A^{DH}, we noted that the α,β-unsaturation and flat conformations of some residues may lead to extended π-electron conjugation. Consequently, we measured the UV-visible absorption spectrum of A^{DH}_{68} in HFIP and compared this to an α-helical sample of poly(L-alanine)$_{53}$, A_{53}, in HFIP as a control. Contrary to A_{53}, which has only weak amide absorption above 200 nm, A^{DH}_{68} showed a strong absorption maximum at 220 nm with absorption extending to nearly 300 nm (Figure 4a). The absorption of A^{DH}_{68} in this region is due to the known spectroscopic properties of Dha residues.[74] The fluorescence spectra of both samples were also acquired. The A_{53} sample in HFIP showed weak absorption (λ_{max} = 302 nm) and emission (λ_{max} = 400 nm); while A^{DH}_{68} in HFIP showed considerably stronger absorption at higher wavelength (λ_{max} = 354 nm) and a remarkable strong blue emission (λ_{max} = 440 nm) (Figure 4b,c).
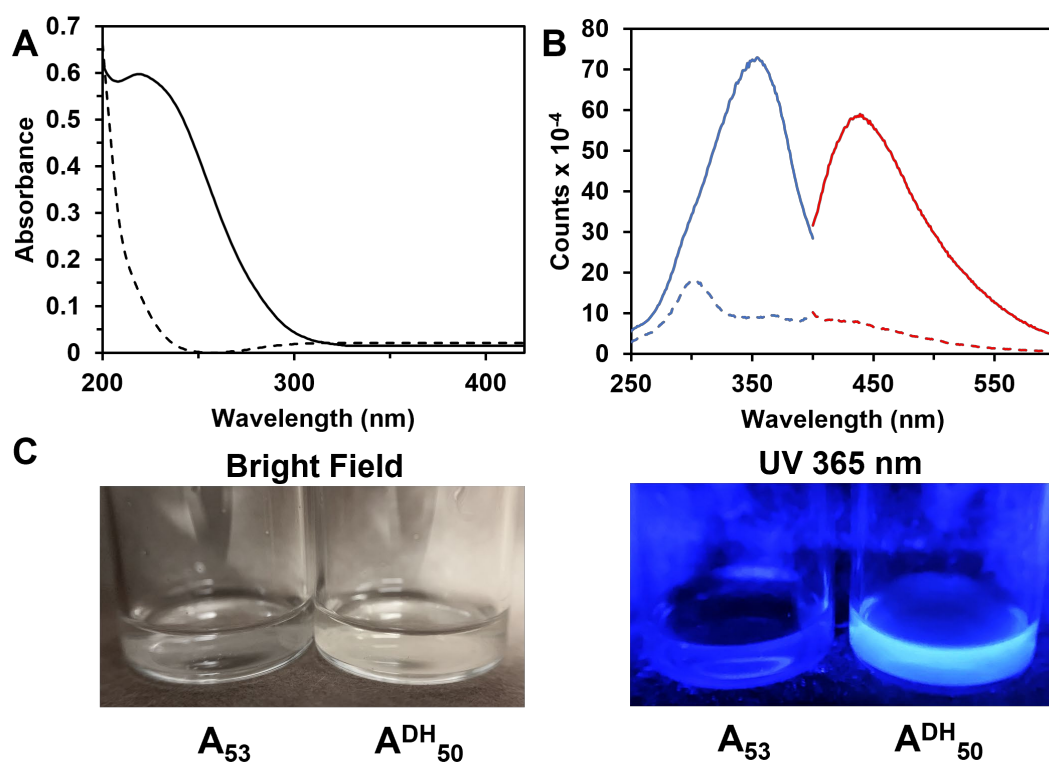

**Figure 4** Spectroscopic properties of A^{DH}_{68} (solid lines) and poly(L-alanine)$_{53}$, A_{53} (dashed lines) in HFIP. A) UV/vis absorption spectra, B) excitation (blue) and emission (red) spectra. All samples were prepared

in HFIP (0.1 mg/mL) and spectra were acquired at 20 ºC. C) Images of $\mathbf{A_{53}}$ and $\mathbf{A^{DH}_{50}}$ at 1.0 mg/mL in HFIP. Left image is under ambient light (bright field), and right image is under UV irradiation at 365 nm.

Seeking to better understand the nature of $\mathbf{A^{DH}}$ fluorescence, we observed that while both of the polypeptides disperse well in HFIP to give limpid samples, we found via dynamic light scattering that both $\mathbf{A_{53}}$ and $\mathbf{A^{DH}_{68}}$ form nanoscale aggregates in this solvent (see SI Figure S6). Consequently, it is likely that the fluorescence properties of these samples arise due to aggregation induced emission (AIE) from the nanoparticles rather than from individual solvated chains.[75,76] While such AIE has been reported for synthetic polypeptides,[75,76] the intrinsic blue fluorescence of $\mathbf{A^{DH}}$ has much higher intensity compared to that observed in other polypeptides in dilute suspension, such as $\mathbf{A_{53}}$ (Figure 4c). The blue fluorescence of $\mathbf{A^{DH}}$ is potentially valuable for the development of label-free polypeptide nanoscale assemblies and biomaterials for combination therapeutic and imaging applications.
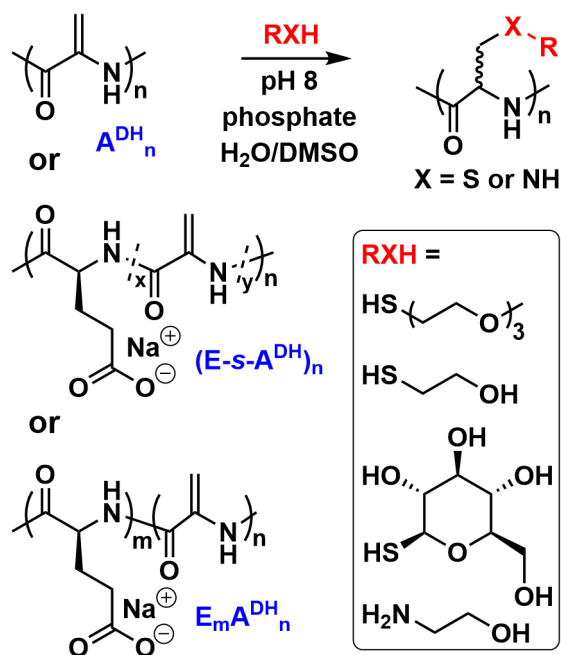
Scheme 6 Functionalization of $\mathbf{A^{DH}}$ containing polypeptides using thiol and amine nucleophiles.

Another feature of Dha containing polypeptides is the ability to functionally modify these residues by reaction with nucleophiles.[5-8] To evaluate the ability to functionally modify residues in $\mathbf{A^{DH}}$, we reacted homo, statistical, and block copolypeptides of $\mathbf{A^{DH}}$ with model thiol and amine nucleophiles in mixtures

of DMSO and water (Scheme 6, Table 2). Addition of DMSO was necessary to disperse the hydrophobic **A**[DH] segments of homo and block copolypeptides in aqueous media. All reactions proceeded in high yields with no sign of peptide chain cleavage (Table 2, see SI), and the use of hydrophilic nucleophiles resulted in fully water soluble products. As expected since the Dha precursors lack stereocenters, the resulting modified Dha residues possessed racemic stereochemistry as verified by circular dichroism spectroscopy (see SI Figure S7).[10] The facile modification of Dha residues in **A**[DH] provides a new effective route to side-chain functional polypeptides, which have promise for development of a diverse range of properties. Since the products of reactions of **A**[DH] with thiol nucleophiles are poly(S-alkyl-DL-cysteines), the racemic nature of these products likely provides an added benefit in enhancing their solubility by disfavoring the β-sheet formation commonly observed in poly(L-cysteine) derivatives.[77] An additional feature provided by modification of Dha residues was reduction of **A**[DH] fluorescence. Monitoring of polypeptide fluorescence at different stages of the reaction of **A**[DH] with mercaptoethanol revealed that fluorescence decreased as a function of residue modification (see SI Figure S8). Thus chemical modification of **A**[DH] can be used to switch chain conformation, solubility, and fluorescence properties.

Table 2. Preparation of functional derivatives of **A**[DH] containing polypeptides

Starting Polymer	Nucleophile	Product	Functionalization (%)[a]	Yield (%)[b]
A^{DH}_{72}	mEG$_3$SH	$(rac\text{-}C^{EG3})_{72}$	>99	86
$(E\text{-}s\text{-}A^{DH})_{67}$	mEG$_3$SH	$[E\text{-}s\text{-}(rac\text{-}C^{EG3})]_{67}$	>99	89
$E_{88}A^{DH}_{85}$	mEG$_3$SH	$E_{88}(rac\text{-}C^{EG3})_{85}$	>99	99
$E_{88}A^{DH}_{85}$	HOEtNH$_2$	$E_{88}(rac\text{-}A^{HEA})_{85}$	>99	98
$E_{88}A^{DH}_{85}$	HOEtSH	$E_{88}(rac\text{-}C^{HE})_{85}$	>99	99
$E_{88}A^{DH}_{85}$	β-D-glcSH	$E_{88}(rac\text{-}C^{GLC})_{85}$	>99	95

[a] Determined by ^{1}H NMR analysis of functionalized polypeptide. [b] Isolated yield of purified polypeptide.

Conclusions

Via the design of a new, soluble poly(L-cysteine) based precursor, we have developed a route for successful preparation of long chain $\mathbf{A^{DH}}$, and the incorporation of Dha residues and $\mathbf{A^{DH}}$ segments into copolypeptides. Based on experimental and computational data, $\mathbf{A^{DH}}$ was found to adopt a previously unobserved 'hybrid coil' structure, which combines elements of both 2_5-helical and 3_{10}-helical conformations. Analysis of the spectroscopic properties of $\mathbf{A^{DH}}$ revealed that it possesses strong inherent blue fluorescence that may be amenable for use in downstream imaging applications. $\mathbf{A^{DH}}$ also contains reactive electrophilic groups that allowed its efficient modification to functionalized polypeptides after reaction under mild conditions with thiol and amine nucleophiles. The combined structural, spectroscopic, and reactivity properties of $\mathbf{A^{DH}}$ make it a unique reactive and fluorescent polypeptide component for utilization in self-assembled biomaterials.

Associated Content

Supporting Information

The Supporting Information is available free of charge on the ACS Publications website at DOI: 10.1021/jacs.#######.

Experimental procedures, spectral data, reaction schemes for copolymerizations and oxidation, additional figures and GPC data (PDF).

Author Information

Corresponding Author

* demingt@seas.ucla.edu

ORCID

Timothy J. Deming: 0000-0002-0594-5025

20

K. N. Houk: 0000-0002-8387-5261

Notes

The authors declare no competing financial interest.

Acknowledgments.

References.

1) Schmidt, U., Lieberknecht, A.; Wild, J. Didehydroamino Acids (DDAA) and didehydropeptides (DDP). *Synthesis* **1988**, 159-172.

2) Humphrey, J. M.; Chamberlin, A. R. Chemical synthesis of natural product peptides: Coupling methods for the incorporation of noncoded amino acids into peptides. *Chem. Rev.* **1997**, *97*, 2243-2266.

3) Palmer, D. E.; Pattaroni, C.; Nunami, K.; Chadha, R. K.; Goodman, M.; Wakamiya, T.; Fukase, K.; Horimoto, S.; Kitazawa, M.; Fujita, H.; Kubo, A.; Shiba, T. Effects of dehydroalanine on peptide conformations. *J. Am. Chem. Soc.* **1992**, *114*, 5634–5642.

4) Crisma, M.; Formaggio, F.; Toniolo, C.; Yoshikawa, T.; Wakamiya, T. Flat peptides. *J. Am. Chem. Soc.* **1999**, *121,* 3272-3278.

5) Fu, S-C. J.; Greenstein, J. P. Saturation of acetyldehydroalanine with benzylamine. *J. Am. Chem. Soc.* **1955**, *77,* 4412-4413.

6) Strumeyer, D. H.; White, W. N.; Koshland Jr., D. E. Role of serine in chymotrypsin action. Conversion of the active serine to dehydroalanine. *Proc. Nat. Acad. Sci. (USA)* **1963**, *50*, 931-935.

7) Zhu, Y.; van der Donk, W. A. Convergent synthesis of peptide conjugates using dehydroalanines for chemoselective ligations. *Org. Lett.* **2001**, *3,* 1189-1192.

8) Ferreira, P. M. T.; Maia, H. L. S.; Monteiro, L. S.; Sacramento, J. Michael addition of thiols, carbon nucleophiles and amines to dehydroamino acid and dehydropeptide derivatives. *J. Chem. Soc. Perkin Trans. 1* **2001**, 3167–3173.

9) Burrage, S.; Raynham, T.; Williams, G.; Essex, J. W.; Allen, C.; Cardno, M.; Swali, V.; Bradley. M. Biomimetic synthesis of lantibiotics. *Chem. Eur. J.* **2000**, *6*, 1455-1466.

10) Chalker, J. M.; Gunnoo, S. B.; Boutureira, O.; Gerstberger, S. C.; Fernández-González, M.; Bernardes, G. J. L.; Griffin, L.; Hailu, H.; Schofield, C. J.; Davis, B. G. Methods for converting cysteine to dehydroalanine on peptides and proteins. *Chem. Sci.* **2011**, *2*, 1666-1676.

11) Yang, A.; Ha, S.; Ahn, J.; Kim, R.; Kim, S.; Lee, Y.; Kim, J.; Söll, D.; Lee, H. Y.; Park, H. S. A chemical biology route to site-specific authentic protein modifications. *Science* **2016**, *354*, 623-626.

12) Dadová, J.; Wu, K-J.; Isenegger, P. G.; Errey, J. C.; Bernardes, G. J. L.; Chalker, J. M.; Raich, L.; Rovira, C. Davis, B. G. Precise probing of residue roles by post-translational β,γ-C,N aza-Michael mutagenesis in enzyme active sites. *ACS Central Sci.* **2017**, *3*, 1168-1173.

13) Freedy, A. M.; Matos, M. J.; Boutureira, O.; Corzana, F.; Guerreiro, A.; Akkapeddi, P.; Somovilla, V. J.; Rodrigues, T.; Nicholls, K.; Xie, B.; Jiménez-Osés, G.; Brindle, K. M.; Neves, A. A.; Bernardes, G. J. L. Chemoselective installation of amine bonds on proteins through aza-Michael ligation. *J. Amer. Chem. Soc.* **2017**, *139*, 18365-18375.

14) Dadová, J.; Galan, S. R.; Davis, B. G. Synthesis of modified proteins via functionalization of dehydroalanine. *Curr Opin Chem Biol.* **2018**, *46*, 71-81.

15) Jones, L. H. Dehydroamino acid chemical biology: an example of functional group interconversion on proteins. *RSC Chem. Biol.* **2020**, *1*, 298-304.

16) Burrage, S. A.; Raynham, T.; Bradley, M. A highly efficient route to dehydroalanine containing peptides. *Tetrahedron Lett.* **1998**, *39*, 2831-2834.

17) Zhu, Y.; Gieselman, M. D.; Zhou, H.; Averin, O.; van der Donk, W. A. Biomimetic studies on the mechanism of stereoselective lanthionine formation. *Org. Biomol. Chem.* **2003**, *1,* 3304-3315.

18) Seebeck, F. P.; Szostak, J. W. Ribosomal synthesis of dehydroalanine-containing peptides. *J. Am. Chem. Soc.* **2006**, *128,* 7150-7151.

19) Morrison, P. M.; Foley, P. J.; Warriner, S. L.; Webb, M. E. Chemical generation and modification of peptides containing multiple dehydroalanines. *Chem. Commun.* **2015**, *51*, 13470-13473.

20) Sakakibara, S. Studies on dehydroalanine derivatives. I. Synthesis of N-carboxy-dehydroalanine anhydride. *Bull Chem. Soc. Jpn.* **1959**, *32*, 13-17.

21) Sakakibara, S. Studies on dehydroalanine derivatives. II. Synthesis of polydehydroalanine. *Bull Chem. Soc. Jpn.* **1960**, *33*, 814-818.

22) Sakakibara, S. Studies on dehydroalanine derivatives. V. Radical polymerization of N-carboxy-dehydroalanine anhydride and of N-phthaloyl-dehydroalanine. Synthesis of a new amphoteric polymer. *Bull Chem. Soc. Jpn.* **1961**, *34*, 174-177.

23) Nandel, F. S.; Malik, N.; Singh, B.; Jain, D. V. S. Conformational structure of peptides containing dehydroalanine: Formation of β-bend ribbon structure. *Int. J. Quantum Chem.* **1999**, *72*, 15-23.

24) Zanuy, D.; Casanovas, J.; Alemán, C. The conformation of dehydroalanine in short homopeptides: molecular dynamics simulations of a 6-residue chain. *Biophys. Chem.* **2002**, *98*, 301-312.

25) Deming, T. J. Synthesis and self-assembly of well-defined block copolypeptides via controlled NCA polymerization. *Adv. Polymer Sci.* **2013**, *262*, 1-37.

26) Deming, T. J. Cobalt and iron initiators for the controlled polymerization of α-amino acid-N-carboxyanhydrides. *Macromolecules* **1999**, *32*, 4500-4502.

27) Walter, R.; Roy, J. Selenomethionine, a potential catalytic antioxidant in biological systems. *J. Org. Chem.* **1971**, *36*, 2561-2563.

28) Rich, D. H.; Tam, J. P.; Mathiaparanam, P.; Grant, J. A.; Mabuni, C. General synthesis of didehydroamino-acids and peptides. *J. Chem. Soc. Chem. Commun.* **1974**, *0*, 897-898.

29) Rich, D. H.; Tam, J. P. Synthesis of didehydropeptides from peptides containing 3-alkylthio-amino acid residues. *Tetrahedron Lett.* **1975**, *16*, 211-212.

30) Rich, D. H.; Tam, J. P. Synthesis of dehydroamino acids and peptides by dehydrosulfenylation. Rate enhancement using sulfenic acid trapping agents. *J. Org. Chem.* **1977**, *42*, 3815-3820.

31) Nomoto, S.; Sano, A.; Shiba, T. A new synthetic method for dehydroalanine peptides through hofmann degradation of α,β-diaminopropionyl residue. *Tetrahedron Lett.* **1979**, *20*, 521-522.

32) Miller, M. J. Isourea-mediated preparation of dehydro amino acids. *J. Org. Chem.* **1980**, *45*, 3131-3132.

33) Okeley, N. M.; Zhu, Y.; van der Donk, W. A. Facile chemoselective synthesis of dehydroalanine-containing peptides. *Org. Lett.* **2000**, *2*, 3603-3606.

34) You, Y. O.; Levengood, M. R.; Ihnken, L. A. F.; Knowlton, A. K.; van der Donk, W. A. Lacticin 481 synthetase as a general serine/threonine kinase. *ACS Chem. Biol.* **2009**, *4*, 379-385.

35) Ramapanicker, R.; Mishra, R.; Chandrasekaran, S. An improved procedure for the synthesis of dehydroamino acids and dehydropeptides from the carbonate derivatives of serine and threonine using tetrabutylammonium fluoride. *J. Peptide Sci.* **2010**, *16*, 123-125.

36) Deming, T. J. Synthesis of side-chain modified polypeptides. *Chem. Rev.* **2016**, *116*, 786–808.

37) Hayakawah, T.; Nishi, H.; Noguchi, J.; Ikeda, S.; Yamashita, T.; Isemeura, T. The synthesis of protein analogue. XXIII-XXV. XXIV. The syntheses of ω-benzyl esters of α-amino-α, co-dicarboxylic acids and the properties of their polymers. *Nippon kagaku zassi* **1961**, *82*, 601–604.

38) Harrap, B. S.; Stapleton, I. W. Poly-S-carbobenzoxymethyl-l-cysteine: A model system for the denaturation of non-helical proteins. *Biochim. Biophys. Acta* **1963**, *75*, 31-36.

39) Ikeda, S.; Maeda, H.; Isemura, T. The β-structure of poly-S-carbobenzoxymethyl-l-cysteine in solution. *J. Mol. Biol.* **1964**, *10*, 223-234.

40) Xiao, J.; Li, M.; Liu, W.; Li, Y.; Ling, Y.; Tang, H. Synthesis and thermoresponsive properties of poly(L-cysteine)s bearing imidazolium salts. *Eur. Poly. J.* **2017**, *88*, 340-348.

41) Xiao, J.; Tan, J.; Jiang, R.; He, X.; Xu, Y.; Ling, Y.; Luan, S.; Tang, H. A pH and redox dual responsive homopolypeptide: synthesis, characterization, and application in "smart" single-walled carbon nanotube dispersion. *Polym. Chem.* **2017**, *8*, 7025-7032.

42) Hayakawa, T.; Kondo, Y.; Murakami, Y. Syntheses and conformational studies of poly(S-aminoalkyl-L-cysteines) and their benzyloxycarbonyl derivatives. *Polym. J.* **1974**, *6*, 424–430.

43) Liu, H.; Wang, R.; Wei, J.; Cheng, C.; Zheng, Y.; Pan, Y.; He, X.; Ding, M.; Tan, H.; Fu, Q. Conformation-directed micelle-to-vesicle transition of cholesterol-decorated polypeptide triggered by oxidation. *J. Amer. Chem. Soc.* **2018**, *140*, 6604-6610.

44) Frankel, M.; Zilkha, A. Synthesis of poly-S-allylcysteine (poly-deoxo-alliin). *Nature* **1955**, *175*, 1045–1046.

45) Hayakawa, T; Matsuyama, M.; Inoue, K. Poly (S-alkyI-L-cysteines) containing long aliphatic side chains. *Polymer* **1977**, *18*, 854-855.

46) Fu, X.; Shen, Y.; Fu, W.; Li, Z. Thermoresponsive oligo(ethylene glycol) functionalized poly-l-cysteine. *Macromolecules* **2013**, *46*, 3753–3760.

47) Akbulut, H.; Yamada, S.; Endo, T. Phosgene-free synthesis of poly(l-cysteine) containing styrene moiety as a reactive function. *Macromol. Chem. Phys.* **2017**, *218*, 1700078.

48) Yi, L.; Wang, Y.; Lin, G.; Lin, D.; Chen, W.; Huang, Y.; Ye, G. Synthesis of conformation switchable cationic polypeptides based on poly (S-propargyl-cysteine) for use as siRNA delivery. *Int. J. Biol. Macromol.* **2017**, *101*, 758-767.

49) Hayakawa, T.; Kondo, Y.; Matsuyama, M. Syntheses and conformational studies of poly (S-menthyloxycarbonylmethyl L-and D-cysteines). *Polymer* **1976**, *17*, 1009-1012.

50) Kramer, J. R.; Deming, T. J. Glycopolypeptides with a redox-triggered helix-to-coil transition. *J. Amer. Chem. Soc.* **2012**, *134*, 4112-4115.

51) Ikeda, S.; Fasman, G. D. Optical rotatory dispersion of poly-S-carboxymethyl-l-cysteine in aqueous solutions: A beta ⇌ random coil transition. *J. Mol. Biol.* **1967**, *30*, 491-505.

52) Ikeda, S. Molecular conformation of poly-S-carboxymethyl-L-cysteine in aqueous solutions. *Biopolymers* **1967**, *5*, 359-374.

53) Ikeda, S.; Fukutome, A.; Imae, T.; Yoshida, T. Circular dichroism and the pH-induced β-coil transition of poly(S-carboxymethyl-L-cysteine) and its side-chain homolog. *Biopolymers* **1979**, *18*, 335-349.

54) Holmes, T. J.; Lawton, R. G. Cysteine modification and cleavage of proteins with 2-methyl-N1-benzenesulfonyl-N4-bromoacetylquinonediimide. *J. Amer. Chem. Soc.* **1977**, *99*, 1984-1986.

55) Włostowski, M.; Czarnocka, S.; Maciejewski, P. Efficient S-alkylation of cysteine in the presence of 1,1,3,3-tetramethylguanidine. *Tetrahedron Lett.* **2010**, *51*, 5977-5979.

56) Lavilla, C.; Byrne, M.; Heise, A. Block-sequence-specific polypeptides from α-amino acid N-carboxyanhydrides: Synthesis and influence on polypeptide properties. *Macromolecules* **2016**, *49*, 2942-2947.

57) Bonduelle, C. Secondary structures of synthetic polypeptide polymers. *Polym. Chem.* **2018**, *9*, 1517-1529.

58) Kramer, J. R.; Onoa, B.; Bustamante, C.; Bertozzi, C. R. Chemically tunable mucin chimeras assembled on living cells. *Proc. Nat. Acad. Sci. (USA)* **2015**, *112*, 12574-12579.

59) Aujard-Catot, J.; Nguyen, M.; Bijani, C.; Pratviel, G.; Bonduelle, C. Cd 2+ coordination: an efficient structuring switch for polypeptide polymers. *Polym. Chem*. **2018**, *9*, 4100–4107.

60) Kramer, J. R.; Deming, T. J. Multimodal switching of conformation and solubility in homocysteine derived polypeptides. *J. Amer. Chem. Soc.* **2014**, *136*, 5547–5550.

61) Noda, K.; Gazis, D.; Gross, E. Solid-phase synthesis of peptides via alpha, beta-unsaturated amino acids: oxytocin, simultaneous incorporation of amide functions in COOH-terminal and endo-positions. *Int. J. Pept. Protein. Res.* **1982**, *19*, 413-419.

62) Younis, I. R.; Elliott, M.; Peer, C. J.; Cooper, A. J. L.; Pinto, J. T.; Konat, G. W.; Kraszpulski, M.; Petros, W. P.; Callery, P. S. Dehydroalanine analog of glutathione: An electrophilic busulfan metabolite that binds to human glutathione S-transferase A1-1. *J. Pharmacol. Exp. Ther.* **2008**, 327, 770-776.

63) Henzler Wildman, K. A.; Ramamoorthy, A.; Wakamiya, T.; Yoshikawa, T.; Crisma, M.; Toniolo, C.; Formaggio, F. A study of a $C^{\alpha,\beta}$-didehydroalanine homo-oligopeptide series in the solid-state by ^{13}C cross-polarization magic angle spinning NMR. *J. Peptide Sci.* **2004**, *10*, 336-341.

64) Siodłak, D.; Macedowska-Capiga, A.; Broda, M. A.; Kozioł, A. E.; Lis, T. The cis-trans isomerization of N-methyl-α,β-dehydroamino acids. *Biopolymers* **2012**, *98*, 466-478.

65) Malek, K.; Makowski, M.; Królikowska, A.; Bukowska, J. Comparative studies on IR, Raman, and surface enhanced Raman scattering spectroscopy of dipeptides containing ΔAla and ΔPhe. *J. Phys. Chem. B* **2012**, *116*, 1414−1425.

66) Peggion, C.; Moretto, A.; Formaggio, F.; Crisma, M.; Toniolo, C. Multiple, consecutive, fully-extended 2.0$_5$-helix peptide conformation. *Biopolymers* **2013**, *100*, 621-636.

67) Katchalski, E.; Sela, M.; Silman, H. I.; Berger, A. Polyamino acids as protein models. In *The Proteins Composition, Structure, and Function, Volume 2*; Neurath, H., Ed.; Academic Press: New York, **1964**; pp 405–601.

68) Avignon, M. Huong, P. V.; Lascombe, J.; Marraud, M. Neel, J. Etude, par spectroscopie infrarouge, de la conformation de quelques composés peptidiques modèles. *Biopolymers* **1969**, *8*, 69–89.

69) Toniolo, C. Intramolecularly hydrogen-bonded peptide conformations. *Crit. Rev. Biochem.* **1980**, *9*, 1–44.

70) Burgess, A. W.; Scheraga, H. A. Stable conformations of dipeptides. *Biopolymers* **1973**, *12*, 2177–2183.

71) Scheiner, S. Relative strengths of NH••O and CH••O hydrogen bonds between polypeptide chain segments. *J. Phys. Chem. B* **2005**, *109*, 16132-16141.

72) Newberry, R. W.; Raines, R. T. A prevalent intraresidue hydrogen bond stabilizes proteins. *Nat. Chem. Biol.* **2016**, *12*, 1084-1088.

73) Grimme, S. Exploration of chemical compound, conformer, and reaction space with meta-dynamics simulations based on tight-binding quantum chemical calculations. *J. Chem. Theory Comput.* **2019**, *15*, 2847−2862.

74) Carter, C. E.; Greenstein, J. P. Spectrophotometric determination of dehydropeptidase activity. *J. Natl. Cancer Inst.* **1946**, *7*, 51-56.

75) Ye, R.; Liu, Y.; Zhang, H.; Su, H.; Zhang, Y.; Xu, L.; Hu, R.; Kwok, R. T. K.; Wong, K. S.; Lam, J. W. Y.; Goddard, III, W. A.; Tang, B. Z. Non-conventional fluorescent biogenic and synthetic polymers without aromatic rings. *Polym. Chem.* **2017**, *8*, 1722-1727.

76) Chen, X.; Luo, W.; Ma, H.; Peng, Q.; Yuan, W. Z.; Zhang, Y. Prevalent intrinsic emission from nonaromatic amino acids and poly(amino acids). *Sci. China Chem.* **2018**, *61*, 351–359.

77) Bauer, T. A.; Muhl, C.; Schollmeyer, D.; Barz, M. Racemic S-(ethylsulfonyl)-dl-cysteine N-carboxyanhydrides improve chain lengths and monomer conversion for β-sheet-controlled ring-opening polymerization. *Macromol. Rapid Commun.* **2021**, *42*, 2000470.

TOC Graphic: